The Shape of Sound: a Geometric Morphometrics Approach to Laryngeal Functional Morphology

Heather L Borgard, Karen Baab, Bret Pasch & Tobias Riede

Journal of Mammalian Evolution

ISSN 1064-7554

J Mammal Evol
DOI 10.1007/s10914-019-09466-9

Journal of Mammalian Evolution
https://doi.org/10.1007/s10914-019-09466-9

ORIGINAL PAPER

The Shape of Sound: a Geometric Morphometrics Approach to Laryngeal Functional Morphology

Heather L Borgard[1] · Karen Baab[2] · Bret Pasch[3] · Tobias Riede[1]

Abstract

Diversification of animal vocalizations plays a key role in behavioral evolution and speciation. Vocal organ morphology represents an important source of acoustic variation, yet its small size, complex shape, and absence of homologous landmarks pose major challenges to comparative analyses. Here, we use a geometric morphometric approach based on geometrically homologous landmarks to quantify shape variation of laryngeal cartilages of four rodent genera representing three families. Reconstructed cartilages of the larynx from contrast-enhanced micro-CT images were quantified by variable numbers of three-dimensional landmarks placed on structural margins and major surfaces. Landmark sets were superimposed using generalized Procrustes analysis prior to statistical analysis. Correlations among pairwise Procrustes distances were used to identify the minimum number of landmarks necessary to fully characterize shape variation. We found that the five species occupy distinct positions in morphospace, with variation explained in part by phylogeny, body size, and differences in vocal production mechanisms. Our findings provide a foundation for quantifying the contribution of vocal organ morphology to acoustic diversification.

Keywords Source-filter theory · Bioacoustics · Rodents · Ventral pouch · Vocal production

Introduction

Divergence in acoustic signals that mediate mate recognition and social interactions is thought to play an important role in the diversification of many animals (Bradbury and Vehrencamp 2011; Wilkins et al. 2013). In mammals, different factors contribute to acoustic variation. First, central nervous system control of respiration and movement of the larynx and vocal tract determines how aerodynamic energy is converted into sound (e.g., Jürgens 2009). In addition, laryngeal and vocal tract morphology influence acoustic properties by determining how sound transfers in the vocal tract and radiates from the lips or nares (e.g., Titze 2000). Identifying the relative contributions of each component to acoustic variation is critical to understanding the evolution of vocal communication systems.

The larynx is located at the crossroads of the alimentary and respiratory tract and serves multiple functions including respiration and sound production. The cartilaginous framework of the larynx (Negus 1949; Harrison 1995) plays an important role in vocal fold tension and positioning control (Hunter and Titze 2005). In particular, laryngeal muscles move thyroid, cricoid, and arytenoid cartilages in order to regulate vocal fold posture and length, two variables that determine fundamental frequency (Riede 2013; Titze et al. 2016). Although the diversity of laryngeal morphology within (Schild 1984; Ajmani 1990; Eckel et al. 1994; Eckel and Sittel 1995; Sprinzl et al. 1999; Tayama et al. 2001; Jain and Dhall 2008; Jotz et al. 2014; Loth et al. 2015) and between species (Negus 1949; Schneider 1964; Denny 1976; Harrison 1995) has been described, its functional association with species-specific vocal behavior is understudied. Previous attempts to quantify laryngeal morphology have been hampered by its complex structure and the absence of discrete landmarks that can be identified across taxa. The geometric morphometrics approach quantifies shape from corresponding curves and

✉ Tobias Riede
triede@midwestern.edu

[1] Department of Physiology, Midwestern University, 19555 N 59th Ave, Glendale, AZ 85308, USA

[2] Department of Anatomy, Midwestern University, 19555 N 59th Ave, Glendale, AZ 85308, USA

[3] Department of Biological Sciences, Northern Arizona University, 617 S. Beaver St, Flagstaff, AZ 86011, USA

Published online: 02 May 2019

surfaces (Rohlf 1999; Klingenberg 2008; Adams et al. 2013), and facilitates comparative analyses even with few homologous landmarks. Herein, we present the first application of geometric morphometric techniques to investigate larynx functional morphology to enhance current efforts using linear dimensions (Storck and Unteregger 2018).

Many new discoveries highlight the importance of vocal behavior in social interactions of rodents (e.g., Shelley and Blumstein 2004; Pasch et al. 2011; Rieger and Marler 2018). Furthermore, rodents represent the most speciose mammalian order (Macdonald and Norris 2001) and are model organisms in biomedical research (e.g., Shu et al. 2005). While rodents represent one of the most widely tractable mammalian groups, their vocal organ is complex and relatively small in size. However, recent developments in imaging technology have made such structures accessible to morphological reconstruction (Metscher 2009; Clarke et al. 2016; Riede et al. 2017). The goal of this work is to investigate shape variation of a complex morphological structure within a comparative framework.

Acoustic features of vocalizations are often more similar in closely related species (e.g., Cap et al. 2008; Luo et al. 2017; Miller and Engstrom 2012). Thus, we explored whether acoustic similarities among muroid rodents are associated with variation in laryngeal shape. We used landmark analysis to quantify laryngeal shape in five rodent species that differ in properties of their social vocalizations (Fig. 1). We acquired three-dimensional (3D) landmarks and semilandmarks from the laryngeal cartilages to quantify homologous curves and surfaces (Gunz and Mitteroecker 2013). As our study is the first landmark-based analysis of larynx shape, we also evaluated the minimum landmark / semilandmark density required to quantify the primary variation in each of the four major laryngeal cartilages (McLeod 2015). Our study represents an initial step in a larger investigation of the form-function relationship between larynx shape and vocalizations. As this is a novel approach to larynx morphology, the goals are in part exploratory – identifying shape features that discriminate among species – and in part practical – establishing a workflow that can be applied to a larger comparative sample of rodents.

Methods

Animals and Micro-CT Imaging

Investigations were performed in two murid species (four house mice, *Mus musculus*, CD1 strain, two/sex; and four laboratory rats, *Rattus norvegicus*, Sprague Dawley strain, two/sex), two cricetid species (four male grasshopper mice; two *Onychomys arenicola*, two *O. leucogaster*), and one heteromyid species (four kangaroo rats; *Dipodomys ordii*; two/sex). All specimens were processed at Midwestern University, Glendale, AZ. Experimental procedures were in accordance with the National Institutes of Health guidelines for experiments involving vertebrate animals and were approved by the Institutional Animal Care and Use Committee at Midwestern University, Glendale, AZ (protocol #2478). Grasshopper mice and kangaroo rats were captured with approval from the Arizona Game and Fish Department (#SP763978).

Larynges were dissected and fixed in 10% buffered formalin phosphate (SF100–4; Fisher Scientific) for 24 h. Each specimen was stained with iodine (Riede et al. 2017). Stained specimens were placed in a custom-made acrylic tube and scanned in air with 59 kV source voltage and 167 μA intensity using a Skyscan 1172 (Bruker-microCT, Kontich, Belgium). Projection images were recorded with an angular increment of 0.4° over a 180° rotation. Voxel size in the reconstructed volumes was 5.03 μm per pixel. Reconstructed image stacks were then imported into AVIZO software (version Lite 9.0.1). Laryngeal cartilages and the border between the airway and soft tissues of the larynx in the CT scans were traced manually to provide an outline of the cartilaginous framework. Derived three-dimensional (3D) surfaces (STL format) and video animations of all specimens are available on Morphobank (O'Leary and Kaufman 2012), project 2686 (Riede et al. 2017).

Landmark Selection

Each 3D landmark is comprised of a set of x, y, and z coordinates acquired from a location that can be identified reliably across individuals and taxa. A classic categorization of landmarks recognizes three main types (Bookstein 1991). Type I landmarks are biologically homologous points located at the juxtaposition of tissue types (e.g., intersection of cranial sutures). Type II landmarks are geometrically defined at local maxima or minima (e.g., tip of a bony or cartilaginous process). Finally, Type III landmarks are extremal points defined by the position of other landmarks or an external coordinate system and thus have at least one 'deficient' coordinate. Semilandmarks are Type III landmarks positioned along homologous curves or surfaces where discrete landmarks cannot be identified (Bookstein 1997; Gunz and Mitteroecker 2013; Wärmländer et al. 2019). In this study, both Type II and III landmarks were utilized to define the shape of laryngeal cartilages (Table 1 and Fig. 2).

How many landmarks are necessary and sufficient to describe the geometric form of a larynx? There is a minimum number of landmarks and/or semilandmarks required to capture the desired level of biological detail (i.e., comprehensive coverage; Roth and Levine 1993). While more landmarks and semilandmarks provide additional shape information, too many semilandmarks, which are geometrically deficient,

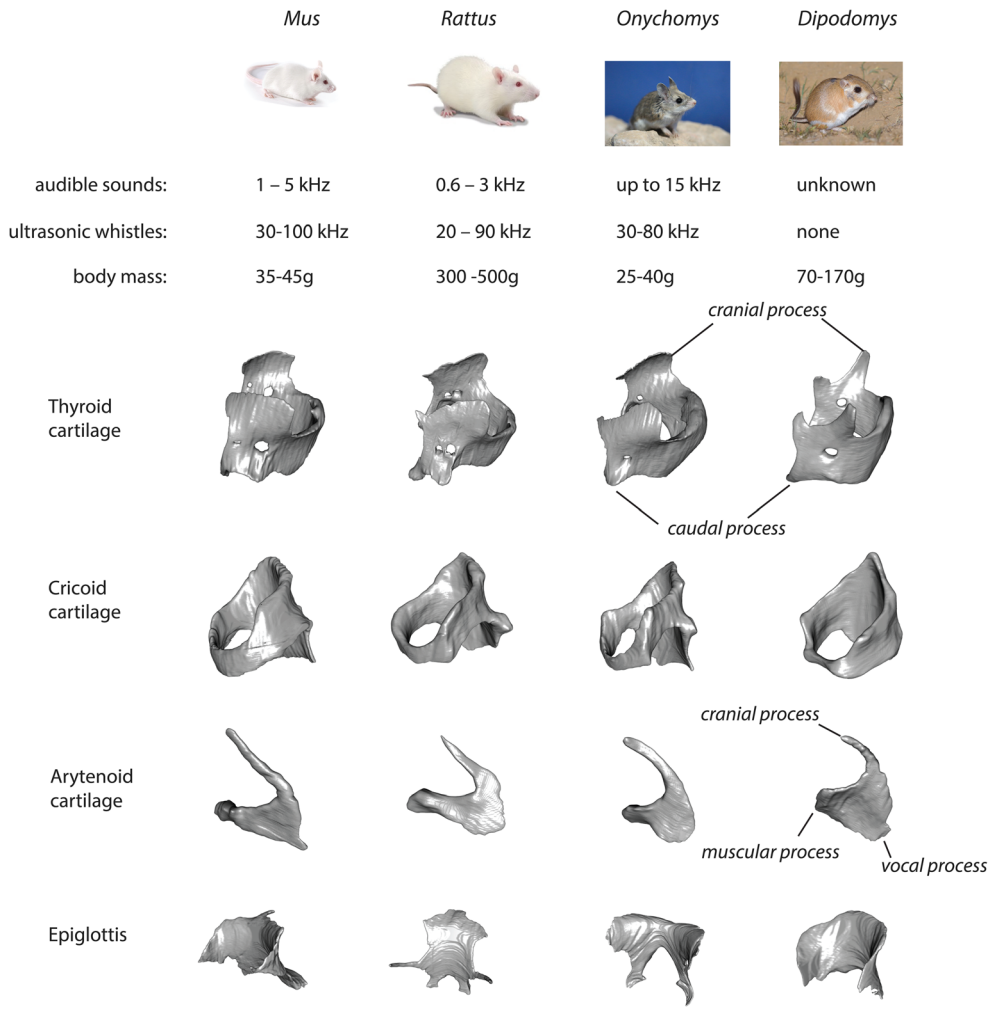

Fig. 1 Representative laryngeal cartilages from each of the four rodent genera as well as information about their vocalization and body size

may disproportionately influence the analysis (e.g., Zelditch et al. 2004). Moreover, there are likely diminishing returns in the amount of information gained by adding more semilandmarks. Therefore, we also evaluated how increasing the number of landmarks / semilandmarks affected the pattern of shape similarity among individuals by calculating pairwise distances for increasingly dense (semi)landmark sets (Fig. 2).

Shape Analysis

We first analyzed shape using only fixed landmarks and curve semilandmarks, and subsequently added surface semilandmarks to the analysis. All landmarks and semilandmarks were placed on surface renderings generated from the CT data in the 'geomorph' package, Version 3.0.5. (Adams et al. 2017) for the R software package (R Development Core Team 2017). Fixed landmarks (explained in Table 1) were supplemented by an increasing number of sliding curve semilandmarks that were placed along the cartilage border between the fixed landmarks. Both types of curve landmarks were placed manually ("digit.fixed" function in 'geomorph') and surface semilandmarks were placed with help of an interactive function to build a template of 3D surface semilandmarks ("buildtemplate"). All semilandmarks were 'slid' into positions of geometric homology across specimens by minimizing the bending energy matrix with regard to the reference based on the assumption that the underlying morphology is homologous, even if individual points are not (Bookstein 1997; Bookstein et al. 2002; Gunz and Mitteroecker 2013).

The coordinate data were superimposed using generalized Procrustes analysis (GPA) for each set of (semi)landmarks analyzed (Gower 1975; Rohlf and Slice 1990). The GPA process removes variation related to position, size, and orientation by a) translating specimens' centroids (geometric center) to the origin, b) scaling all configurations to unit centroid size (defined as the square root of the sum of Euclidean distances from all landmarks to the centroid), and c) rigidly rotating the data to minimize distances across all corresponding landmarks in an iterative procedure (e.g., Baab et al. 2012). The superimposed coordinates reflect differences in shape that

Table 1 Definition of type II, i.e. fixed curve landmarks on laryngeal cartilages. Sliding semilandmarks (type III) were added between those landmarks

Thyroid cartilage	
1	Posterior most point on rostral margin of left cranial process
2	Midline point on cranial margin
3	Posterior most point on cranial margin of right cranial process
4	Posterior most point on caudal margin of right caudal process
5	Midline point on caudal margin
6	Posterior most point on caudal margin of left caudal process
Cricoid cartilage	
1	Posterior most point on cranial margin
2	Most left point on cranial margin
3	Anterior most point on cranial margin
4	Most right point on cranial margin
5	Posterior most point on caudal margin
6	Most left point on caudal margin
7	Anterior most point on caudal margin
8	Most right point on caudal margin
Arytenoid cartilage	
1	Most distal point on cranial process
2	Most distal point on vocal process
3	Most distal point on muscular process
Epiglottis	
1	Most cranial point along midsagittal line
2	Most left point on lateral margin
3	Most caudal point along midsagittal line
4	Most right point on lateral margin

are invariant with regard to position, orientation, and size, but exist in a non-Euclidean shape space. Thus, the data were projected onto a Euclidean tangent space in order to utilize standard multivariate statistical approaches. Procrustes distance, calculated here as Euclidean distance in the tangent space (Rohlf 1999), summarizes shape differences between two superimposed landmark configurations.

We generated 120 pairwise Procrustes distances among all 16 specimens based on a small number of landmarks and semilandmarks. These distances were re-calculated based on incrementally increased numbers of (semi)landmarks, and Pearson correlation coefficients among these distances were used to evaluate the optimal number of (semi)landmarks. The higher the correlation coefficient, the less additional information was gained by additional landmarks. A correlation coefficient of 1.0 indicates identical distances among landmark configurations and thus no additional shape information was gained. We analyzed curve and surface semilandmarks separately alongside the fixed curve landmarks.

Statistical Analysis

We employed a series of principal components analyses (PCA), an effective data reduction technique, to summarize the main patterns of shape variance in the data. We also present PCAs for different numbers of landmarks to illustrate their effect on the interpretation of among-species differences. Shape variation along PC axes were generated by first identifying the specimen closest to the mean shape and then warping it to the mean shape using the "warpRefMesh" function in Geomorph. The loadings for each PC axis were added and subtracted from the mean shape to produce the shapes at the positive and negative ends of each axis, respectively, using the "PlotTangentSpace" function in 'geomorph'. We used single-linkage clustering of species mean scores from the first two PCs to compare the pattern of among-species shape similarities across cartilages and visualized these using dendograms (calculated in SPSS), and performed multivariate analysis of variance (MANOVA) on the PC 1 and PC 2 score for each cartilage to determine whether species were statistically distinguishable on the basis of cartilage shape.

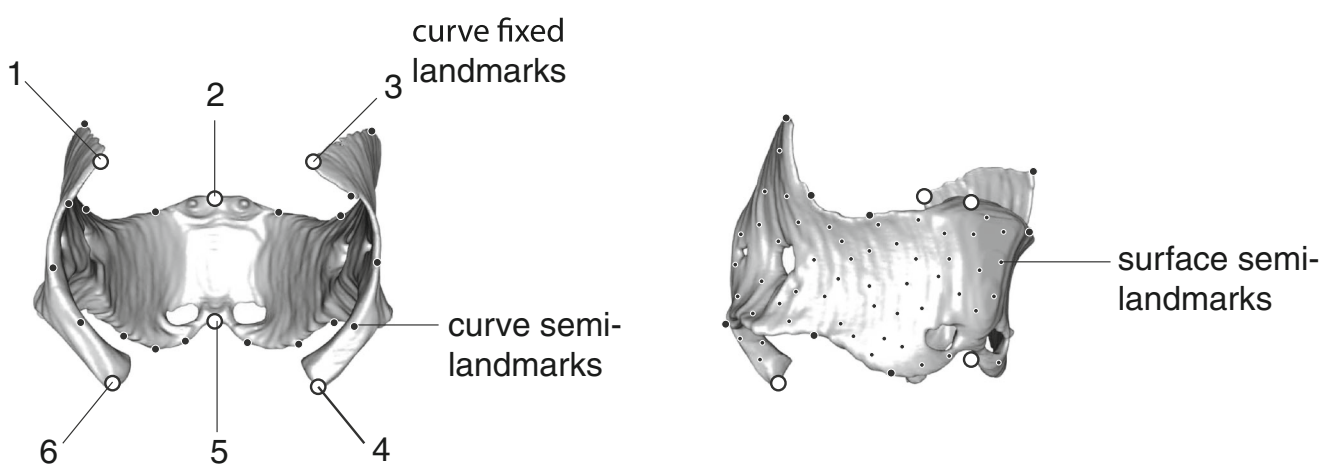

Fig. 2 Exemplary image of a thyroid cartilage with six curve fixed landmarks (1 through 6, for definitions see Table 1), 24 curve semilandmarks and some of the 100 surface semilandmarks. Curve semilandmarks were free to slide along their curve

Data Availability

The datasets analyzed during the current study (stl files of all cartilages) are available in the Morphobank repository, https://morphobank.org/index.php/Projects/ProjectOverview/project_id/2686.

Results

Number of Landmarks

The curve semilandmarks are defined for each cartilage in Table 1. The correlation coefficients of pairwise Procrustes distances based on increasing numbers of curve landmarks are presented in Fig. 3a-d. The curve landmarks were doubled in three steps. Correlations increased at first and then plateaued.

The correlation coefficients of pairwise Procrustes distances based on increasing numbers of surface landmarks (5, 10, 20, 30, 40, 50, 100) are presented in Fig. 3e-h. As expected, correlation coefficients became saturated as more semilandmarks were added. The correlation coefficients of the Procrustes distances surpassed 0.90 with 20 landmarks and leveled off at about 0.97 with ≥40 semilandmarks for the thyroid, cricoid, and arytenoid cartilages (Fig. 3a-d). There was not much new shape information gained beyond 24 semilandmarks for the thyroid cartilage. For the epiglottis,

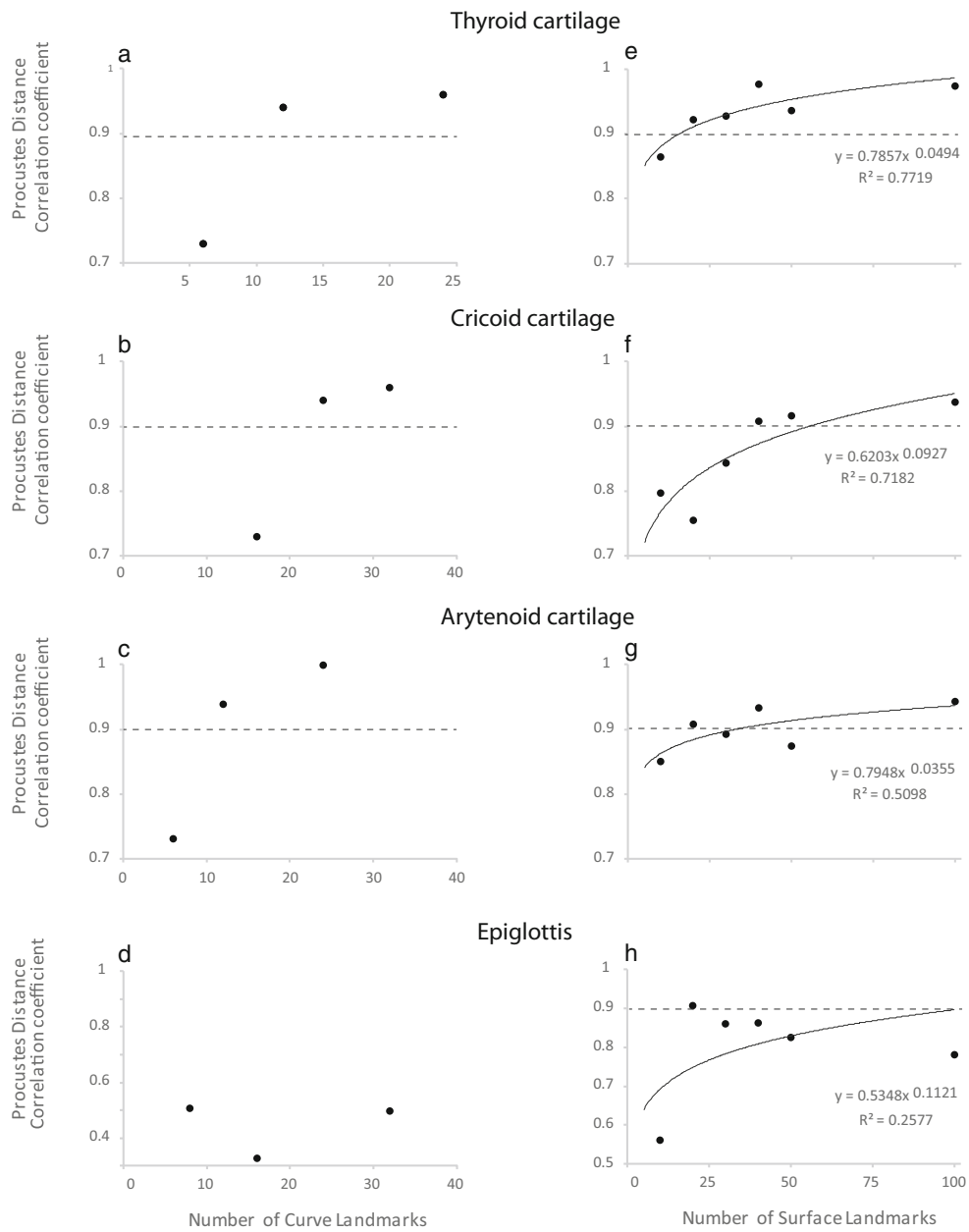

Fig. 3 Pairwise Procrustes distances among all 16 individuals (120 pairs) were calculated using curve (**a-d**) and surface (**e-h**) landmarks. **a-d** For thyroid cartilage, arytenoid cartilage and epiglottis, the correlations between Procrustes distances for 3 and 6 curve landmarks (as well as 6 vs. 12; 12 vs. 24), respectively, are shown. For the cricoid cartilage, correlations between 8 vs. 16; 16 vs. 24; 24 vs. 32, curve landmarks were analyzed. **e-h** The correlation between Procrustes distances for 5 and 10 surface landmarks (as well as 10 vs. 20; 20 vs 30; 30 vs 40; 40 vs 50; 50 vs 100), respectively. The dotted horizontal lines at 0.9 are an arbitrarily chosen threshold

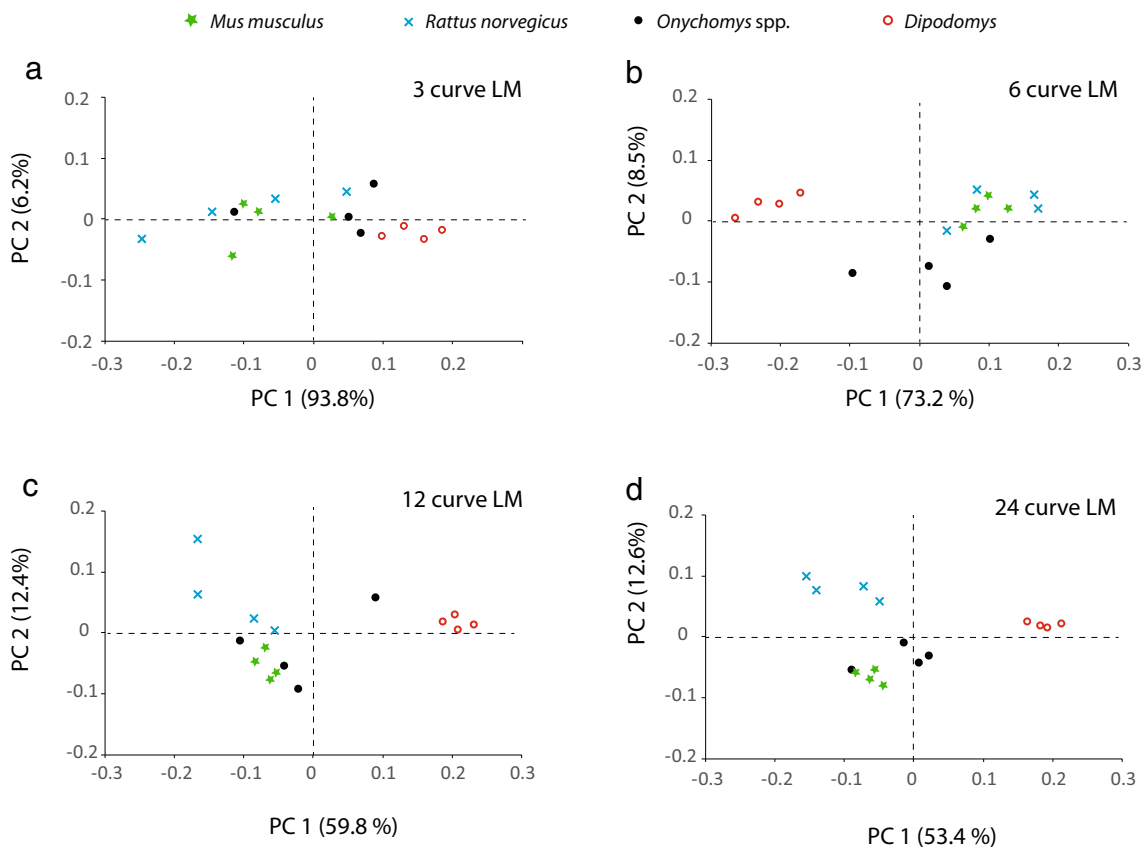

Fig. 4 Ordination of PC scores of Procrustes shape coordinates using 3 (**a**), 6 (**b**), 12 (**c**), and 24 (**d**) curve landmarks (LM) on the thyroid cartilage. Note that kangaroo rats (*Dipodomys*) separate from the three muroid rodents even with three landmarks. Differentiation among the three muroid rodents increases as more landmarks are used

the coefficient barely reached 0.90 using 20 surface landmarks and remained below 0.90 when larger numbers of landmarks were used.

We also performed PCAs to visualize how varying numbers of semilandmarks would affect the position of individuals in morphospace. The results are exemplified for curve semilandmarks of the thyroid cartilage in Fig. 4. Results of the PCA analyses of different curve landmark numbers indicated that kangaroo rats (*Dipodomys*) clustered separately from the three muroid rodents even with only three landmarks. Different patterns of interspecific variation among the three muroid rodents were apparent on PC 2 in the 6 versus the 12 and 24 landmark sets (Fig. 4b, c). Group differences stabilized at 12 landmarks, but were clearest when 24 landmarks were used (Fig. 4d). Results for cricoid and arytenoid cartilages were similar – larger landmark numbers improved species separation. The epiglottis shape variation showed fewer species-specific patterns.

Interspecific Morphospace Variation

Next, we investigated how the 16 specimens clustered in morphospace using the optimal number of curve and surface semilandmarks based on the previous assessment (Fig. 5). The five species exhibited strong separation of their thyroid shape along the first principal component (PC) (Fig. 5a). The four kangaroo rats clustered on the positive end of PC 1 opposite from the muroid rodents, likely due to a laterally widened cartilage and very narrow and pointed rostral horn (Fig. 6a). The second PC for the thyroid cartilage analysis separated the two larger species (*Rattus* and *Dipodomys*) from the two smaller muroids (*Mus* and *Onychomys*) (Fig. 5a, b). The larger species had a more obtuse angle between the caudal processes and the laminae, which allows greater rotation of the thyroid around the crico-arytenoid joint.

The first and second PCs of the cricoid cartilage differentiated the three muroid rodents from each other (Fig. 5c, d). The kangaroo rat specimens clustered near the origin on both axes. The shape of the cross-sectional area of the air column appears "pinched" dorsally and there was a reduced craniocaudal height of the dorsal lamina and lateral surface in species that scored high on PC 1 (*Mus* and *Rattus*) (Fig. 6d). High scoring species on PC 2 (*Rattus*) had a dorsoventrally elongated cross-section, an oblique dorsal lamina, and a vertically short lateral surface (Fig. 6e). The third PC describes variation of the length of the dorsal lamina such that a long caudal projection (below the facet for the thyroid cartilage) was characteristic of high-scoring specimens (mostly *Rattus*) (Fig. 6f).

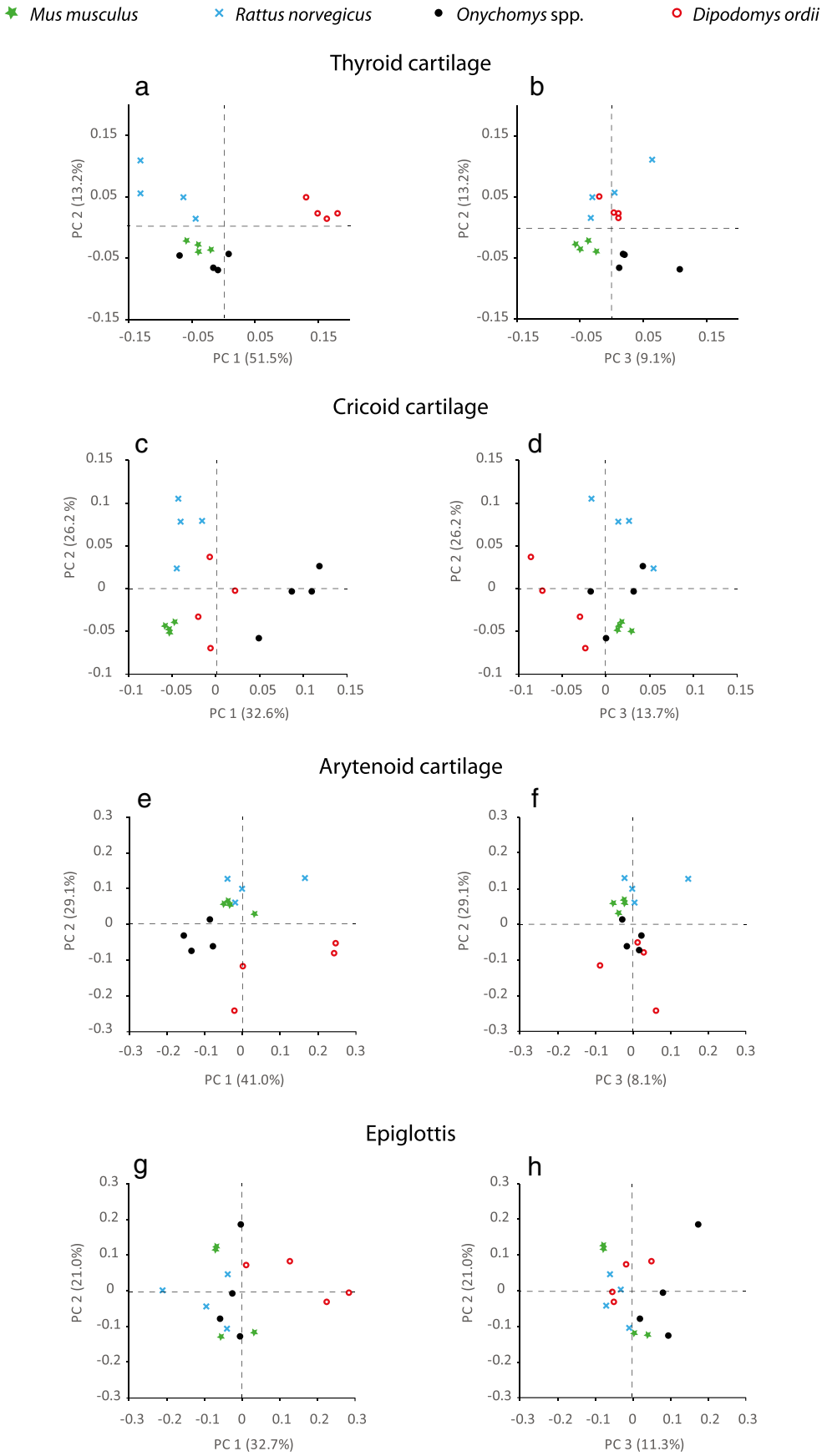

Fig. 5 Principal component analysis of the Procrustes shape coordinates from curve and surface semilandmarks. Each point represents the cartilage shape of an individual. The first and second principal components (PC) (**a**, **c**, **e**, **g**) and second and third PCs (**b**, **d**, **f**, **h**) are shown. Note that axis scaling differs between cartilages

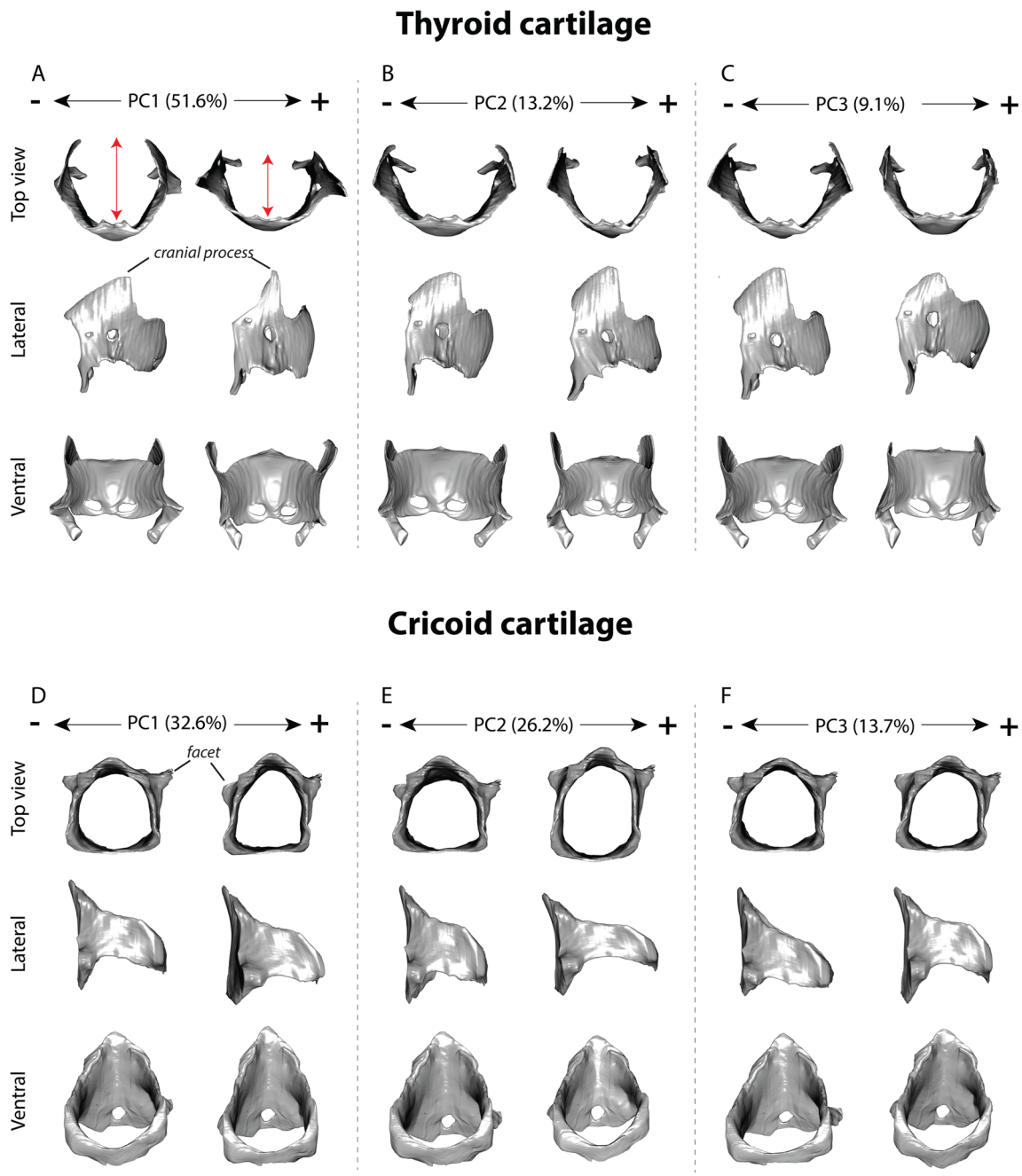

Fig. 6 **a-f** Warped cartilage images showing shape changes. Images represent shape changes associated with the minimum and maximum extents of PC1, PC2, and PC3 for the thyroid (**a-c**), cricoid (**d-f**), arytenoid (**g-i**) cartilages and epiglottis (**i-l**)

Grasshopper mice and kangaroo rats were most distinct in the subspace of the first two PCs of the arytenoid cartilage shape (Fig. 5e, f). Grasshopper mice, situated at the negative end of PC 1, were characterized by a long dorsal process and a relatively shorter distance between vocal and muscular processes (Fig. 6g). The arytenoid body is relatively large at the negative end of PC 2 (kangaroo rat) but smaller on the positive end (laboratory rat and mouse). The third PC captured less then 10% of the variation, but provided some additional separation between laboratory rats and mice.

Next, we investigated whether any particular laryngeal cartilage represented a more sensitive indicator of interspecific differences. The results of the MANOVA indicated that the four genera were statistically distinguishable in their thyroid ($F_{4,\ 16} = 47.2$, $p < 0.001$; Wilk's $\Lambda = 0.007$; partial $\eta^2 = 0.91$), cricoid ($F_{4,\ 16} = 18.9$, $p < 0.001$; Wilk's $\Lambda = 0.026$; partial $\eta^2 = 0.84$), arytenoid ($F_{4,\ 16} = 11.7$, $p < 0.001$; Wilk's $\Lambda = 0.057$; partial $\eta^2 = 0.76$), and epiglottis ($F_{4,\ 16} = 3.2$, $p = 0.02$; Wilk's $\Lambda = 0.28$; partial $\eta^2 = 0.46$) shape. Partial η^2 values suggest that the epiglottis does not discriminate among species as well as the other cartilages.

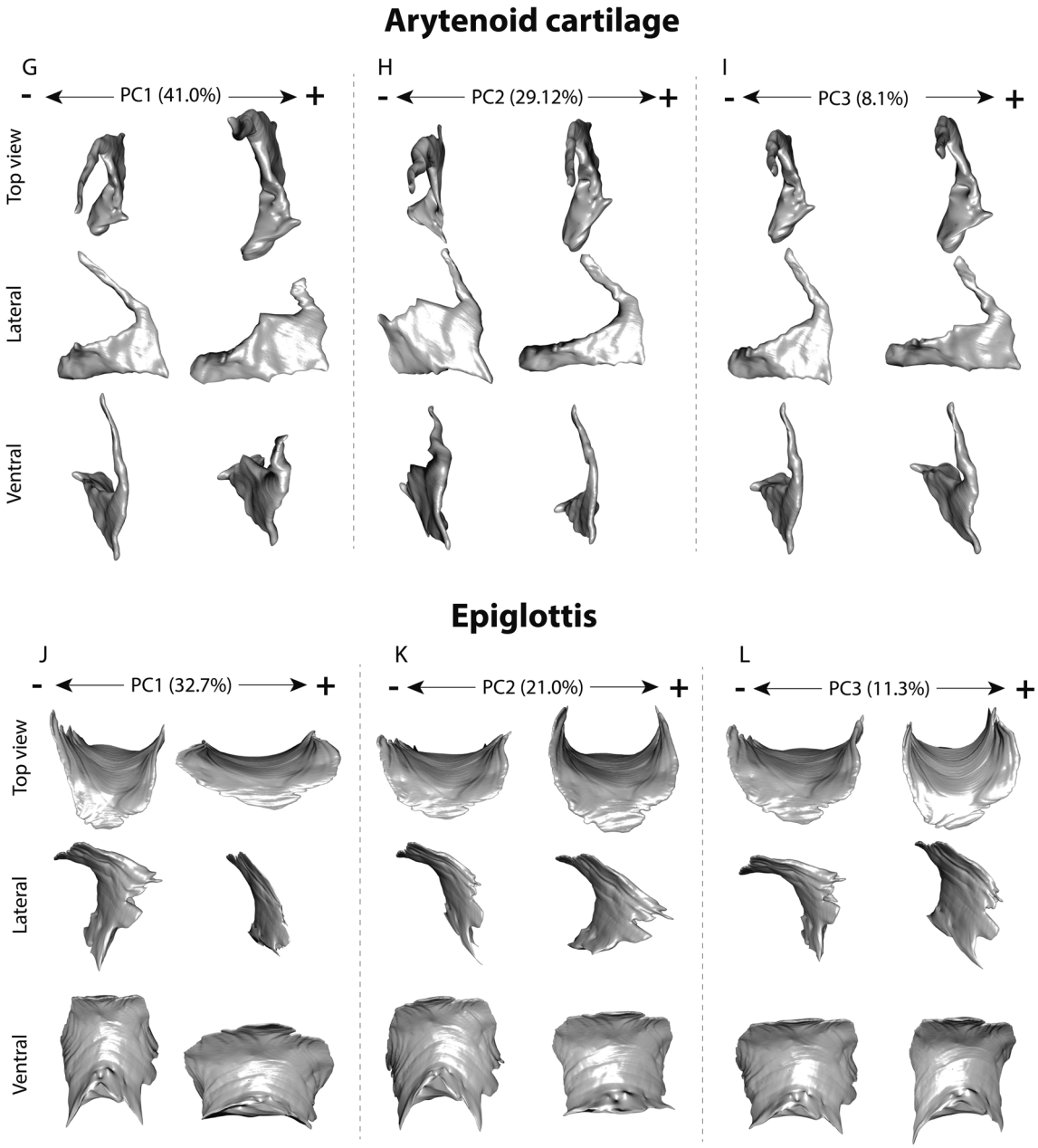

Fig. 6 (continued)

We clustered groups based on their dissimilarity scores for each cartilage (Fig. 7). The first two PCs always separated kangaroo rats from the muroid rodents, reflecting phylogenetic relationships and functional differences. The proximity and topology of shape similarity within muroid rodents differed among the four cartilages, which may reflect functional trade-offs for breathing and/or vocal production. Arytenoid topology reflected phylogenetic relatedness, but thyroid and epiglottis topologies were consistent with body size (Fig. 7). Interestingly, the dissimilarity score was much lower for the cricoid cartilage than the other three cartilages, indicating strong constraints. The lower dissimilarity scores for the cricoid cartilage is consistent with the observation that the PC 1 scores fall in a tighter range for this cartilage compared to the other cartilages. The lower dissimilarity scores for the cricoid cartilage compared to the other three cartilages suggests that cricoid shape is more constrained, at least for the two primary dimensions of shape.

In order to inform the structure-function association, we compared the orientation of three of the cartilages relative to each other. We found a more pinched dorsal cricoid in grasshopper mice. Fig. 8 demonstrates the position of the arytenoid cartilage in 3D models of segmented larynges. The arytenoid cartilage articulates with the cricoid cartilage in a similar

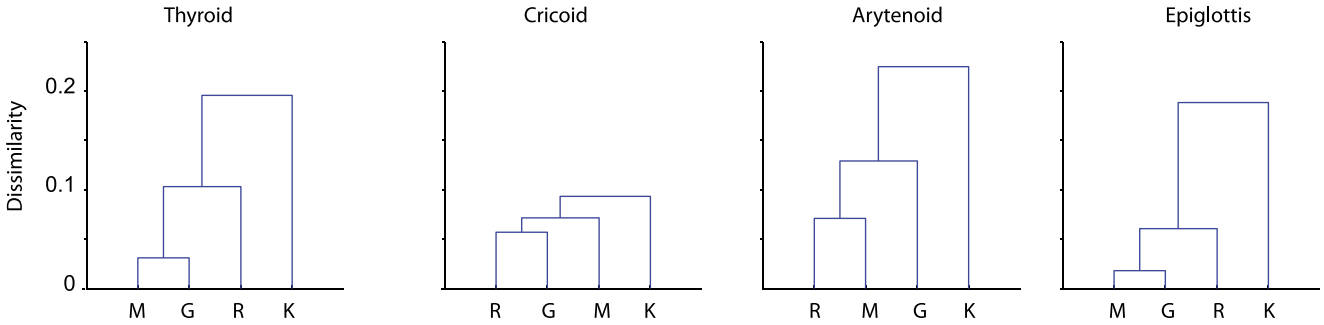

Fig. 7 Pair-wise dissimilarity of laryngeal cartilages among four genera of rodents. The vertical axis of the dendrograms represents the dissimilarity score between the four genera (M, *Mus musculus*; R, *Rattus norvegicus*; G, *Onychomys* spp.; K, *Dipodomys ordii*). Dendrograms were generated from species centroids of the first and second principle component using nearest neighbor clustering

fashion in all four genera. The cartilage sits cranially on the cricoid and does not point more or less dorsally in any species.

Discussion

Our findings indicate that mice have species-specific morphologies of laryngeal cartilages. Interestingly, the greatest divergence in laryngeal morphospace was between species that commonly produce ultrasonic vocalizations and one that rarely does (Randall 1994; Holy and Guo 2005; Brudzynski 2005; Pasch et al. 2017). This result is seemingly at odds with Roberts' (1975) conclusion that ultrasonic vocal production is not associated with laryngeal specializations. Furthermore, species differences in laryngeal anatomy among the muroid rodents diverged in a manner that corresponds with structural characteristics of vocalizations. We discuss our findings in relation to our ultimate goal of linking morphology and function.

Number of Landmarks

Our results indicate a saturation effect with increasing numbers of morphological landmarks. Twenty landmarks recovered the same major patterns of species differentiation as the full landmark set and distances among individuals measured with the reduced and full landmark sets were highly positively correlated. However, small protrusions or depressions with potential functional importance may be undersampled by the sliding landmarks method and thus represent an ongoing challenge (e.g., Botton-Divet et al. 2015). For example, the articular facet of the caudal thyroid horn sits on a prominent lateral process of the cricoid cartilage in the muroid rodents but is flat on the lateral lamina of the cricoid in the kangaroo rat (Fig. 1). The warping image shows that this feature is not incorporated into any of the shape variation axes (Fig. 6d-f). Instead, a prominent process like in muroid rodents is visible on all three axes. We infer that an equal distribution of sliding surface landmarks has led to an under-sampling of functionally relevant areas. Moving forward, we suggest that one possible solution is to add fixed landmarks on key areas (e.g., the center of the articular facet for the caudal thyroid horn) to facilitate comparative analyses.

Interspecific Morphospace Variation

The four rodent genera showed considerable variation in the shape of laryngeal cartilages. Landmark-based analysis effectively captured morphological differences in all four cartilages that separated muroid larynges from that of a heteromyid rodent. Distinct characters included a pointed dorsal process of the thyroid cartilage, a smaller and rounder cross-section of the intralaryngeal airway, and the absence of prominent lateral process on the articular facet of the caudal thyroid horn in the kangaroo rat (Fig. 1). The pairwise dissimilarity measures for each cartilage revealed different associations among the three muroid rodent species (Fig. 7). As all three muroid rodents produce both audible and ultrasonic vocalizations (Pasch et al. 2017), we hypothesize that a large laryngeal morphospace facilitates similar functional outcomes.

Functionally, the broad rostral horn (Fig. 6a, 'lateral view') and greater dorso-ventral length of the thyroid cartilage (Fig. 6a, 'top view') creates a relatively large supraglottal space for the ventral pouch of muroid rodents. The ventral pouch is a laryngeal air sac rostral from the vocal folds and is formed by soft tissue whose entrance is reinforced by the alar cartilage. This pouch is critical for ultrasonic vocalizations produced by a whistle mechanism as airflow passes through the glottis and interacts with the alar edge of the entrance hole of the ventral pouch (Riede et al. 2017; Riede 2018). In contrast, the heteromyid rodent has a pointed rostral horn, a relatively small dorsoventral length, and a small supraglottal space that does not contain a ventral pouch. The smaller supraglottic space and absence or underdevelopment of the ventral pouch correlates with the lack of ultrasonic vocalization in the heteromyid rodent, thus supporting a link between laryngeal cartilage morphology and vocalization.

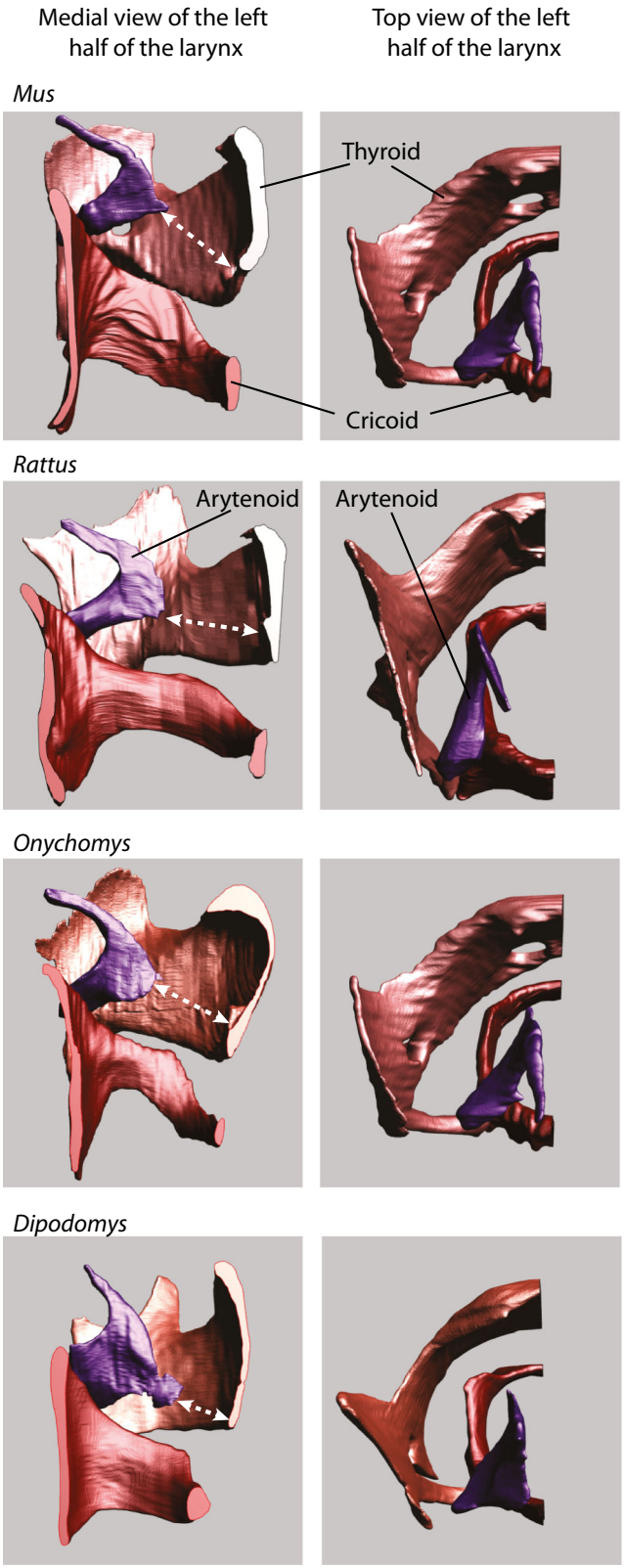

Fig. 8 The arytenoid cartilage articulates with the cricoid cartilage through the crico-arytenoid joint. A dorsal rotation of the arytenoid by contraction of the dorsal crico-arytenoid muscle would elongate and tension the vocal fold (white dashed line). Shape differences in the cricoid and thyroid cartilage of grasshopper mice (*Onychomys* spp.) result in a more dorsally pinched laryngeal airway associated with a more dorsal position of the articular facet. Reconstructions in all four genera suggests a similar orientation of the arytenoid cartilage. STL files for all cartilages and the airway can be viewed on Morphobank

The primary axis of variation of the cricoid cartilage differentiated laboratory rats and mice from grasshopper mice. Such shape variation within muroid rodents is associated with a functional difference. All three muroid species produce ultrasonic whistles but differ in their vocal repertoire below 20 kHz. Whereas *Rattus* and *Mus* produce few audible sounds that are neither complex nor loud (Jourdan et al. 1995), *Onychomys* produce long-distance calls that are exceptionally loud and reach into an unusually high fundamental frequency range of up to 15 kHz (Pasch et al. 2017). Such calls are novel because vocal folds need to be actively positioned and stretched to very high tension in order to reach high vibration rates (Titze et al. 2016; Brown and Riede 2017). Thus, cricoid cartilage shape may contribute to a more robust laryngeal framework (Hunter et al. 2004) that helps support the production of high vocal fold tensions and ultimately high-pitched, loud audible sounds. We hypothesize that the greater dorsal orientation of the aryteno-cricoid facet could facilitate movement of the arytenoid cartilage by orienting more dorsally (i.e. "pull back") in order to achieve high vocal fold tension (e.g., Frable 1961; Von Leden and Moore 1961; Sellars and Keen 1978; Storck et al. 2011). Although the arytenoid cartilage articulation appears similar among the four genera based on 3D geometry of laryngeal cartilage in situ, formalin fixation may alter such positioning. Thus, future studies would benefit from segmentation of the surrounding musculature to better inform biomechanical capabilities. In addition, in vivo scanning could aid in understanding the dynamic character of such laryngeal movements (e.g., Unteregger et al. 2017).

Future Directions

While the results presented herein provide interesting patterns, our small sample size and relatively narrow comparative framework prohibits robust interpretations. Inferring vocal function from laryngeal shape requires consideration of the larynx as a complex multi-segmented structure that integrates different functions related to breathing and feeding. For example, the kangaroo rat larynx has a long, pointed cranial horn and a large, lateral thyroid laminae that provide an attachment surface for extrinsic laryngeal muscles. The articular facets for the caudal thyroid horns on the cricoid cartilage are not prominent in both groups. Although the kangaroo rat larynx has no known vocal function, its unique mode of locomotion (bipedal saltation; Bartholomew and Caswell 1959) may impose mechanical constraints that require locomotor-respiratory

integration (Bramble and Carrier 1983). Vertebral modifications such as a shortening and compaction of the cervical region, a pronounced hyperextension of the neck, and a partial fusion of the anterior neck vertebrae (Hatt 1932) may also be associated with adaptations of the laryngeal valve. Similarly, the laryngeal skeleton is suspended cranially by muscles and ligaments from the hyoid framework and the base of the skull, and caudally by the trachea, bronchi, lungs, and muscles from the sternum. Extrinsic laryngeal musculature acts like a frame in which the larynx is suspended (Vilkman et al. 1996), and stresses generated by vertical respiratory excursions and musculature during swallowing and/or locomotion may stabilize the larynx position and constrain the shape of the thyroid and cricoid cartilages.

Likewise, facial and cranial features may influence laryngeal position and shape (e.g., domestic dogs; Plotsky et al. 2016), indicating that selection unrelated to vocal production may impose fundamental constraints. In rodents, cranial morphology is highly adapted to feeding ecology (Samuels 2009; Pergrams and Lawler 2009). Grasshopper mice possess elongated skulls (Langley 2008) and enlarged coracoid and pterygoid processes that serve as attachment sites for muscles that enable greater bite forces required for their predatory, carnivorous lifestyle (Bailey and Sperry 1929; Satoh and Iwaku 2006; Williams et al. 2009). Thus, future comparative efforts will need to incorporate diet and other ecological factors into multiparametric space to control for their potential indirect effects on laryngeal morphology and vocal repertoire.

In addition to biological considerations, technical improvements of our approach are needed to improve strength of inference. First, segmentation of laryngeal cartilaginous and other soft tissue in small, complex organs remains labor intensive and cost-prohibitive, leading to a relatively small sample size. Furthermore, our findings are restricted to only cartilaginous tissue. Future work would benefit from simultaneous analysis of soft laryngeal tissue including intrinsic muscles and the vocal ligament. Nevertheless, the present study demonstrates the feasibility and benefits of a 3D landmark approach compared to traditional linear measurements in understanding the functional morphology of the larynx.

Conclusion

Laryngeal morphology offers a unique opportunity to study the relationship between form and function in relation to diversification of acoustic signals. When paired with computational simulations (Hunter and Titze 2005; Moisik and Gick 2017), virtual exploration of the morphospace (Palaparthi et al. 2014) promises to provide important insight into the anatomy and mechanisms underlying vocal specialization and divergence. Indeed, one fascinating question arising from the current investigation lies in understanding the substantial differences in intraspecific variation among species; whereas inbred laboratory mice exhibited little individual variation in the first three axes of variation for the thyroid, cricoid, and arytenoid cartilages (Fig. 5a-f), the other three wild-captured species showed much larger variation. Understanding the relative contributions of genetic background and the environment on larynx development and morphology (e.g., Tabler et al. 2017; Laitman et al. 2017) will greatly benefit from a novel geometric morphometrics approach (Beasley De et al. 2013; Klingenberg 2015).

Funding The study was supported by the National Science Foundation (award number 1754332).

References

Adams DC, Collyer ML, Kaliontzopoulou A, Sherratt E (2017) Geomorph: software for geometric morphometric analyses. R package version 3.0.5. (https://cran.r-project.org/package=geomorph.). Accessed July 2017

Adams DC, Rohlf FJ, Slice DE (2013) A field comes of age: geometric morphometrics in the 21st century. Hystrix 24:7–14

Ajmani ML (1990) A metrical study of the laryngeal skeleton in adult Nigerians. J Anat 171:187–191

Baab KL, McNulty KP, Rohlf FJ (2012) The shape of human evolution: A geometric morphometrics perspective. Evolutionary Anthropology 21:151-165

Bartholomew GR, Caswell HH (1959) Locomotion in kangaroo rats and its adaptive significance. J Mammal 32:155–169

Bailey V, Sperry C (1929) Life history and habits of grasshopper mice, genus Onychomys. Technical Bulletin Dept Agriculture 145:1-19.

Beasley De AE, Bonisoli-Alquati A, Mousseau TA (2013) The use of fluctuating asymmetry as a measure of environmentally induced developmental instability: a meta-analysis. Ecol Indicat 30:218–226

Bookstein FL (1991) Morphometric Tools for Landmark Data: Geometry and Biology. Cambridge University Press, Cambridge

Bookstein FL (1997) Morphometric Tools for Landmark Data. Morphometry and Biology. Cambridge University Press, Cambridge

Bookstein FL, Streissguth AP, Sampson PD, Connor PD, Barr HM (2002) Corpus callosum shape and neuropsychological deficits in adult males with heavy fetal alcohol exposure. Neuroimage 15:233–251

Botton-Divet L, Houssaye A, Herrel A, Fabre AC, Cornette R (2015) Tools for quantitative form description; an evaluation of different software packages for semi-landmark analysis. PeerJ 3:e1417

Bradbury JW, Vehrencamp SL (2011) Principles of Animal Communication (2nd edition). Sinauer Associates, Sunderland

Bramble DM, Carrier DR (1983) Running and breathing in mammals. Science 219:251–256

Brown CH, Riede T (2017) An introduction to laryngeal biomechanics. In: Brown CH, Riede T (eds) Comparative Bioacoustics: An Overview. Bentham Science Publishers, Oak Park, pp 120–164

Brudzynski SM (2005) Principles of rat communication: quantitative parameters of ultrasonic calls in rats. Behav Genet 35:85–92

Cap H, Deleporte P, Joachim J, Reby D (2008) Male vocal behavior and phylogeny in deer. Cladistics 24:917–931

Clarke JA, Chatterjee S, Li Z, Riede T, Agnolin F, Goller F, Isasi MP, Martinioni DR, Mussel FJ Novas F (2016) Fossil evidence of the avian vocal organ from the Mesozoic. Nature 538:502–505

Denny SP (1976) Comparative anatomy of the larynx. In: Hinchcliffe R, Harrison DNF (eds) Scientific Basis of Otolaryngology. Heinemann, London, pp 536–545

Eckel HD, Sittel C (1995) Morphometry of the larynx in horizontal sections. Am J Otolaryngol 16:40–48

Eckel HE, Sittel C, Zorowka P, Jerke A (1994) Dimensions of the laryngeal framework in adults. Surg Radiol Anat 16:31–36

Frable MA (1961) Computation of motion at the cricoarytenoid joint. Arch Oto-laryngol 73:73–78

Gower JC (1975) Generalized procrustes analysis. Psychometrika 40:33–51

Gunz P, Mitteroecker P (2013) Semilandmarks: a method for quantifying curves and surfaces. Ital J Mammal 24:103–109

Harrison DFN (1995) The Anatomy and Physiology of the Mammalian Larynx. Cambridge University Press, Cambridge

Hatt RT (1932) The vertebral column of ricochetal rodents. Bull Am Mus Nat Hist 63:599–745

Holy TE, Guo Z (2005) Ultrasonic songs of male mice. PLoS Biol 3(12): e386

Hunter E, Titze IR (2005) Individual subject laryngeal dimensions of multiple mammalian species for biomechanical models. Ann Otol Rhinol Laryngol 114:809–818

Hunter EJ, Titze IR, Alipour F (2004) A three-dimensional model of vocal fold abduction/adduction. J Acoust Soc Am 115:1747–1759

Jain M, Dhall U (2008) Morphometry of the thyroid and cricoid cartilages in adults. J Anat Soc India 57:119–123

Jourdan D, Ardid D, Chapuy E, Eschalier A, LeBars D (1995) Audible and ultrasonic vocalization elicited by single electrical nociceptive stimuli to the tail in the rat. Pain 63:237–249

Jotz GP, Stefani MA, Pereira da Costa Fihlo O, Malysz T, Soster PR, Leao HZ (2014) The morphometric study of the larynx. J Voice 28:668–672

Jürgens U (2009) The neural control of vocalization in mammals: a review. J Voice 23:1–10

Klingenberg CP (2008) Novelty and "homology-free" morphometrics: what's in a name? Evol Biol 35:186–190

Klingenberg CP (2015) Analyzing fluctuating asymmetry with geometric morphometrics: concepts, methods, and applications. Symmetry 7: 843–934

Laitman JT, Noden DM, van de Water TR (2014) Formation of the larynx: from Hox genes to critical periods. In: Rubin JS, Sataloff RT, Korovin GS (eds) Diagnosis and Treatment of Voice Disorders. 4th edition. Plural Publishing, San Diego

Langley WM (2008) Grasshopper Mouse: Evolution of a Carnivorous Lifestyle. Lulu Press, Morrisville, NC

Loth A, Corny J, Santini L, Dahan L, Dessi P, Adalian P, Fakhry N (2015) Analysis of hyoid-larynx complex using 3D geometric morphometric. Dysphagia 30:357–354

Luo B, Huang X, Li Y, Lu G, Zhao J, Zhang K, Zhao H, Liu Y, Feng J (2017) Social call divergence in bats: a comparative analysis. Behav Ecol 28:533–540

Macdonald D, Norris S (2001) The New Encyclopedia of Mammals. Oxford University Press, Oxford

McLeod G (2015) Use of landmark and outline morphometrics to investigate thecal form variation in crushed gogiid echinoderms. Palaeoworld 24:408–429

Metscher BD (2009) MicroCT for comparative morphology: simple staining methods allow high-contrast 3D imaging of diverse non-mineralized animal tissues. BMC Physiol 9:1

Miller JR, Engstrom MD (2012) Vocal stereotypy in the rodent genera *Peromyscus* and *Onychomys* (Neotominae): taxonomic signature and call design. Bioacoustics 21:193–213

Moisik SR, Gick B (2017) The quantal larynx: the stable regions of laryngeal biomechanics and implications for speech production. J Speech Language Hear Res 60:540–560

Negus VE (1949). The Comparative Anatomy and Physiology of the Larynx. Grune and Stratton Inc, New York

Palaparthi A, Riede T, Titze IR (2014) Combining multi-objective optimization and cluster analysis to study vocal fold functional morphology. IEEE Trans Biomed Eng 61:2199–2208

Pasch B, George AS, Hamlin HJ, Guillette LJ, Phelps SM (2011) Androgens modulate song effort and aggression in Neotropical singing mice. Horm Behav 59:90–97

Pasch B, Tokuda IT, Riede T (2017) Grasshopper mice employ distinct vocal production mechanisms in different social contexts. Proc Roy Soc Lond B 284:20171158

Plotsky K, Rendall D, Chase K, Riede T (2016) Cranio-facial remodeling in domestic dogs is associated with changes in larynx position. J Anatomy 228:975-983

Pergams ORW, Lawler JJ (2009) Recent and Widespread Rapid Morphological Change in Rodents. PLoS ONE 4:e6452.

R Core Team (2017). R: A language and environment for statistical computing. R Foundation for Statistical Computing, Vienna, Austria. https://www.R-project.org/

Randall JA (1994) Discrimination of footdrumming signatures by kangaroo rats, *Dipodomys spectabilis*. Anim Behav 47:45–54

Riede T (2013) Call type specific motor patterns in rat ultrasound vocalization. J Exp Zool A 319:213–224

Riede T (2018) Peripheral vocal motor dynamics and combinatory call complexity of ultrasonic vocal production in rats. In: Brudzynski S (editor) Handbook of Behavioral Neuroscience. Elsevier 25:45-60

Riede T, Borgard HL, Pasch B (2017) Laryngeal airway reconstruction indicates rodent ultrasonic vocalizations are produced by an edge tone mechanism. R Soc Open Science 4:170976

Rieger NS, Marler CA (2018) The function of ultrasonic vocalizations during territorial defence by pair-bonded male and female California mice. Anim Behav 135:97–108

Roberts LH (1975) The functional anatomy of the rodent larynx in relation to audible and ultrasonic cry production. Zool J Linn Soc 56: 255–264

Rohlf FJ (1999) Shape statistics: Procrustes superimpositions and tangent spaces. J Classif 16:197–223

Rohlf FJ, Slice D (1990) Extension of the Procrustes method for the optimal superimposition of landmarks. Syst Zool 39:40–59

Roth G, Levine MD (1993) Extracting geometric primitives. CVGIP: Image Understanding 58:1–22

Samuels JX (2009) Cranial morphology and dietary habits of rodents. Zool J Linnean Soc 156:864–888

Satoh K, Iwaku F (2006) Jaw muscle functional anatomy in northern grasshopper mouse, *Onychomys leucogaster*, a carnivorous murid. J Morphol 267:987–999

Schild JA (1984) Relationship of laryngeal dimensions to body size and gestational age in premature neonates and small infants. Laryngoscope 94:1284–1292

Schneider R (1964) Der Larynx der Säugetiere. Handbuch der Zoologie 5:1–128

Sellars IE, Keen EN. (1978) The anatomy and movements of the cricoarytenoid joint. Laryngoscope 88:667–674

Shelley EL, Blumstein DT (2004) The evolution of vocal alarm communication in rodents. Behavioral Ecology 16:169–177

Shu W, Cho JY, Jiang Y, Zhang M, Weisz D, Elder GA, Schmeidler J, Gasperi R, Gama Sosa MA, Rabidou D, Santucci AC, Perl D, Morrisey E, Buxbaum JD (2005) Altered ultrasonic vocalization in mice with a disruption in the Foxp2 gene. Proc Natl Acad Sci USA 10:9643–9648

Sprinzl GM, Eckel HE, Sittel C, Pototschnig C, Koebke J (1999) Morphometric measurements of the cartilaginous larynx: an anatomic correlate of laryngeal surgery. Head Neck 21:743–750

Storck C, Juergens P, Fischer C, Wolfensberger M, Honegger F, Sorantin E, Friedrich G, Gugatschka M (2011) Biomechanics of the cricoarytenoid joint: three-dimensional imaging and vector analysis. J Voice 25:406–410

Storck C, Unteregger F (2018) Cricothyroid joint type as predictor for vocal fold elongation in professional singers. Laryngoscope 128: 1176–1181

Tayama N, Chan RW, Kaga K, Titze IR (2001) Geomtric characterization of the laryngeal cartilage framework for the purpose of biomechanical modeling. Ann Otol Rhinol Laryngol 110:1154–1161

Titze IR (2000) Principals of Voice Production. National Center for Voice and Speech, Salt Lake City

Titze IR, Riede T, Mau T (2016) Predicting fundamental frequency ranges in vocalizations across species. PLoS Comp Biol 12:e1004907

Tabler JM, Rigney MM, Berman GJ, Gopalakrishnan S, Heude E, Al-Lami HA, Yannakoudakis BZ, Fitch RD, Carter CM, Vokes SA, Liu KJ, Tajbakhsh S, Egnor SER, Wallingford JB (2017) Cilia-mediated hedgehog signaling controls form and function in the mammalian larynx. eLife 6:e19153.

Unteregger F, Honegger F, Potthast S, Zwicky S, Schiwowa J, Storck C (2017) 3D Analysis of the Movements of the Laryngeal Cartilages During Singing. Laryngoscope 127: 1639–1643

Vilkman E, Sonninen A, Hurme P, Korkko P (1996) External laryngeal frame function in voice production revisited: a review. J Voice 10: 78–92.

Von Leden H, Moore P. (1961) The mechanics of the cricoarytenoid joint. Arch Otolaryngol 73:541–550.

Wärmländer SKTS, Garvin H, Guyomarc'h P, Petaros A, Sholts SB (2019) Landmark Typology in Applied Morphometrics Studies: What's the Point? The Anatomical Record. https://doi.org/10.1002/ar.24005

Wilkins MR, Seddon N, Safran RJ (2013) Evolutionary divergence in acoustic signals: causes and consequences. Trends Ecol Evol 28: 156–166.

Williams SH, Pfeiffer E, Ford S (2009) Gape and bite force in the rodents *Onychomys leucogaster* and *Peromyscus maniculatus*: does jaw-muscle anatomy predict performance? J Morphol 270:1338–1347

Zelditch ML, Lundrigan BL, Garland T Jr (2004) Developmental regulation of skull morphology. I. Ontogenetic dynamics of variance. Evol Dev 6:194–2063